

STEADY-STATE DYNAMOMETER TESTING OF A PASSENGER VAN: COMPARING OPERATION ON GASOLINE AND AQUEOUS ETHANOL

FINAL REPORT

DECEMBER 2004

ITD Agreement 99-166; KLK351

NIATT N04-15

Prepared for

IDAHO TRANSPORTATION DEPARTMENT

Prepared by

NIATT

**NATIONAL INSTITUTE FOR ADVANCED TRANSPORTATION
TECHNOLOGY
UNIVERSITY OF IDAHO**

Jeff Williams

Faculty Supervision: Steven Beyerlein and Judi Steciak

ABSTRACT

Previous research on catalytic igniters and aqueous fueled engines has shown potential for lowering emissions and increasing engine efficiency over conventional engine configurations. To quantify these improvements in a vehicle platform, a transit van was converted to operate on both gasoline and aqueous fuels, with changeover possible in less than one hour. To facilitate these comparisons, this work explored the use of a six mode test matrix surrounding tests on a steady-state chassis dynamometer. Modes were defined to approximate the Federal Test Protocol (FTP) Urban Driving Cycle. Under common road load conditions, gasoline performance and emissions was compared to operation on 90 percent ethanol and 10 percent water. As expected, the ethanol and water mixture required a 30 percent increase in fuel consumption by volume compared to gasoline. At a road load corresponding to 50 mph, Aquanol displayed a significant increase in CO₂ and HC emissions as well as a significant decrease in NO_x and CO emissions compared with gasoline. It is expected that by upgrading the fuel computer for sequential fuel injection, tuning with a wide-band oxygen sensor, and installing a catalytic converter system with lower a light-off temperature, ethanol and water mixtures could perform significantly better with respect to fuel economy and emissions. A major outcome of this work is the impracticality of comparing vehicle operation on multiple fuels using a modal approximation of the FTP driving cycle. Guidelines for a revised testing procedure that gives better insight about steady-state driving and transient vehicle response with a variety of alcohol-water mixtures are proposed for future work.

TABLE OF CONTENTS

1.	Introduction.....	1
1.1	Characteristics of Aquanol Combustion	2
1.2	Multi-fuel transit van	3
1.3	Catalytic Igniter Technology	5
1.4	Modal Testing	6
2	Research Infrastructure	8
2.1	Dynamometer Facility	8
2.2	Cold Starting Modifications.....	15
2.3	Injector Maintenance	16
3	Experimental Design.....	18
3.1	Optical Pyrometer	18
3.2	Fuel Maps.....	20
3.3	Road Load Replication	22
3.4	Exhaust Measurements	23
3.5	Fuel Metering.....	24
4	Results.....	25
4.1	Performance Testing	25
4.2	Emissions Testing	27
5	Conclusions.....	32
6	Recommendations.....	33
6.1	Recommendations for test protocol	33
6.1	Recommendations for dual-fuel platform.....	33

LIST OF FIGURES

Figure 1.1 Dual-fuel 1985 Ford van.	1
Figure 1.2 Plan view of vehicle infrastructure, showing conversion components.	4
Figure 1.3 Components of the ARI catalytic igniter and flame exiting the pre-chamber...	5
Figure 1.4.1 FTP Urban driving cycle	6
Figure 1.4.2 Highway driving cycle	7
Figure 2.1.1 Experimental Equipment used during dynamometer testing.....	9
FIGURE 2.1.2 Removal of the roll cover floor plates using forklift.	9
FIGURE 2.1.3 Removal of the smaller tie-down track floor plates using forklift	10
Figure 2.1.4 Rack to store tie down track floor plates.	10
Figure 2.1.5 Proper location of dynamometer floor plates and order of removal/installation.....	11
Figure 2.1.6 Correct attachment of the chain to the differential housing.	12
Figure 2.1.7 Correct location of rear wheel with respect to roll center	13
Figure 2.1.8 Ratchet straps and chains securing front wheels.	13
Figure 2.1.9 Exhaust ducting attached to tailpipe.....	14
Figure 2.1.10 Patton industrial fan positioned in front of radiator to increase air flow....	15
Figure 2.2.1 600 Watt Napa in-line radiator heater.	16
Figure 2.3.1 Backflushing unit.....	17
Figure 3.2.1. 3-D fuel injector maps from start-up to 5500 rpm.	20
Figure 3.2.2. Fuel injector duration with respect to coolant temperature.	21
Figure 3.2.3. Fuel injector duration with respect to air temperature.....	21
Figure 3.2.4. Tabular representation of fuel map.....	22
Figure 3.5 MAX Machinery 710 fuel metering system.....	24
Figure 4.2.1 Bar chart comparing CO ₂ emissions of gasoline and Aquanol (90/10).	28
Figure 4.2.2 Bar chart comparing CO emissions of gasoline and Aquanol (90/10).	29
Figure 4.2.3 Bar chart comparing NO _x emissions of gasoline and Aquanol (90/10).	29
Figure 4.2.4 Bar chart comparing HC emissions of gasoline and Aquanol (90/10).	30

LIST OF TABLES

Table 1.1 Heating Value of Fuels on Mass and Volume Basis.	3
Table 1.4 Description of the 6-mode points with weighting factors.....	7
Table 3.1.1 Typical header temperatures during operation on gasoline.	19
Table 3.1.2 Typical header temperatures during operation on Aquanol (90/10).....	19
Table 3.4.1 Composition of calibration gas.	23
Table 4.0.1 Measurement Errors for Data Collection Equipment	25
Table 4.1.1 Torque and horsepower over the six modal points.	27
Table 4.2 five-gas emissions of Aquanol and gasoline over the six modal points.	31

1. INTRODUCTION

Accumulation of atmospheric pollutants as well as concerns about depleting fossil fuel reserves has created demand for alternative automotive power sources. The use of alcohol based fuels as an alternative to gasoline is appealing because of the ability to derive these fuels from organic, renewable sources. In other studies, alcohol fuels have shown similar levels of CO and hydrocarbon emissions along with significant decreases in NO_x [Clark, 2001]. This work demonstrates the feasibility of operating a dual-fuel platform to compare the performance and emission characteristics of ethanol/water mixtures versus gasoline. The converted vehicle is shown in Figure 1.1.



Figure 1.1 Dual-fuel 1985 Ford van.

1.1 Characteristics of Aquanol Combustion

Aquanol is a chemically stable blend of alcohol and water. This research focuses on the azeotrope containing ethanol. Similar bond angles and the polarity of both the water and ethanol molecules make them completely miscible in all proportions [Solomons, 1977]. Percentages of the constituents vary for testing, so the composition will be denoted following the term to avoid confusion (i.e., Aquanol (90/10) is 90 percent ethanol, 10 percent water). Ethanol's ability to homogeneously absorb and suspend water makes it a successful component of aqueous fuels. However, this hygroscopic property also makes it difficult to predict the exact composition after exposure to the atmosphere, as it will absorb water from the air to some extent. Currently, blends of 85 percent ethanol and 15 percent gasoline—called E85—are commercially available [Wyman, 1996].

Adding water to ethanol can result in significant reductions of NO_x by decreasing combustion temperatures. However, cold-starting capabilities using Aquanol containing more than 35 percent water are generally poor, and greater dilution will result in incomplete combustion of in-cylinder hydrocarbons [Jehlik, 1999]. Previous work done at the University of Idaho demonstrated the ability of Aquanol-fueled engines to run on mixtures up to 50 percent ethanol and 50 percent water with cold starting capabilities [Morton, 1999].

Another advantage of adding water to ethanol is from an economic perspective. Conventional distillation can produce only about 95 percent pure ethanol, while further purification is done at great expense through a molecular sieve [Bradley, 1984]. Although ethanol costs more than gasoline to produce at this time, net cost is below wholesale gasoline cost as it is taxed at a much lower rate [Ethanol Report, 1998]. Increasing use of ethanol as an oxygenate in reformulated gasoline and as an alternative fuel in some markets will likely decrease the price further as ethanol becomes more economical to produce. Currently about 95 percent of ethanol is produced from agricultural crops [Nadkarni, 2000]. The most common include high-starch crops such as barley, sorghum, and sugarcane. Ethanol can also be produced from paper-mill by-products.

There is a significant difference between Aquanol and conventional fuels in terms of their energy content. This is highlighted in Table 1.1. The lower heating value of Aquanol fuel means that provisions for supplying greater fuel flow rates need to be implemented to match power output. For this reason major modifications to the fuel delivery and metering system were required for this work to proceed.

Table 1.1 Heating Value of Fuels on Mass and Volume Basis.

Fuel	Lower Heating Value on Mass Basis	Lower Heating Value on Volume Basis
Aquanol (90/10)	23.56 MJ/Kg	19.1 MJ/Liter
Ethanol	27 MJ/Kg	21.2 MJ/Liter
Gasoline	43 MJ/Kg	31.8 MJ/Liter

1.2 Multi-fuel transit van

This research employed a demonstration platform that could be used to compare gasoline and Aquanol on a chassis dynamometer. The vehicle, a 1985 Ford Econoline Van, was donated by Valley Transit of Lewiston, Idaho. Conversion of multiple systems in the vehicle (i.e., fuel storage, fuel delivery, electrical wiring and cold starting) involved many considerations not found in an engine-only conversion. Figure 1.2 illustrates the major components involved in this conversion.

Due to lower combustion temperatures, catalytic clean-up of exhaust by a three-way catalyst during operation on Aquanol is not achievable. Although exhaust cleanup was not optimized for operation on Aquanol, conventional three-way catalytic converters were used to verify baseline emissions on gasoline. Results were similar to the stock vehicle.

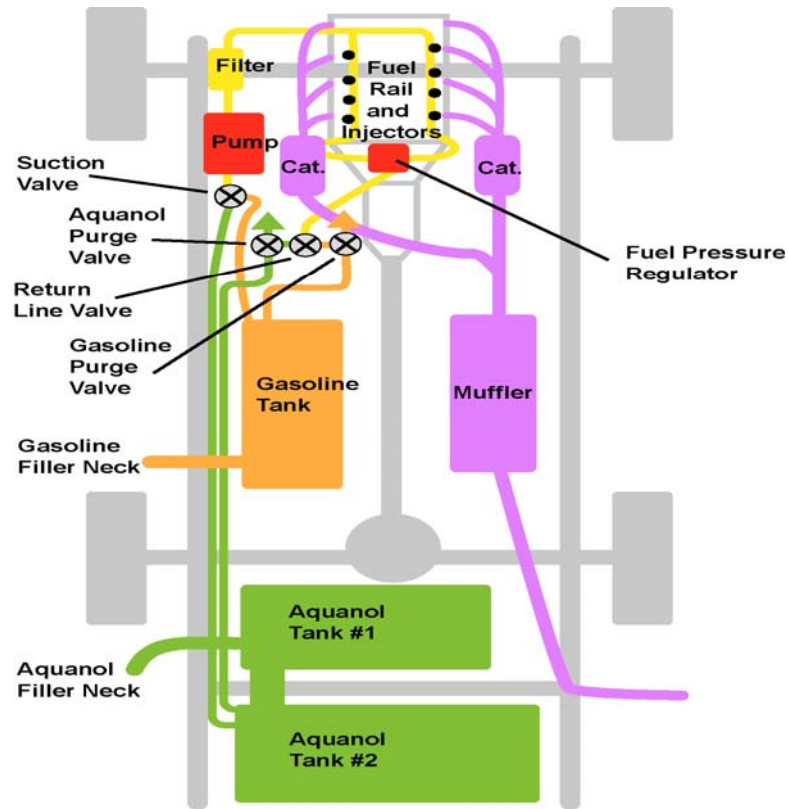


Figure 1.2 Plan view of vehicle infrastructure, showing conversion components.

The vehicle conversion included separate storage for both gasoline and Aquanol. The first Aquanol storage tank used in this research was made of steel with the interior surface coated with teflon®. The teflon was intended to act as a barrier against corrosion.

After two years of use, examination of the fuel tank showed the coating had failed and particles were clogging the remainder of the fuel system. In 2003, the Aquanol handling system was removed and replaced with a polypropylene tank which had anodized fuel pickups. Space is available for a second polypropylene tank that would increase the on-board fuel capacity to 46 gallons. This would provide greater vehicle range than a stock 25-gallon tank containing gasoline. Flexible fuel lines are made with Earls Auto-Flex™ hose consisting of HTE synthetic rubber bonded to a braided stainless steel shell. Rigid fuel lines and fittings are made of 304 grade stainless steel.

1.3 Catalytic Igniter Technology

The primary drawback to Aquanol is the difficulty of initiating and sustaining combustion [Cherry, 1992]. An ignition source using a catalytic reaction in a pre-chamber provides a high-power torch ignition that has proven successful at igniting mixtures previously un-ignitable by spark or compression ignition [Gottschalk, 1995]. Automotive Resources Inc. (ARI) has held the patent on catalytic ignition in a pre-chamber since 1990 [Cherry, 1990]. Over the last decade ARI has made many improvements in the robustness and reliability of catalytic ignition for a variety of engines. This work uses the ARI catalytic igniters to initiate combustion of Aquanol. Figure 1.3 provides an exploded view of the ARI catalytic igniter along with a typical torch ignition emanating from the igniter.

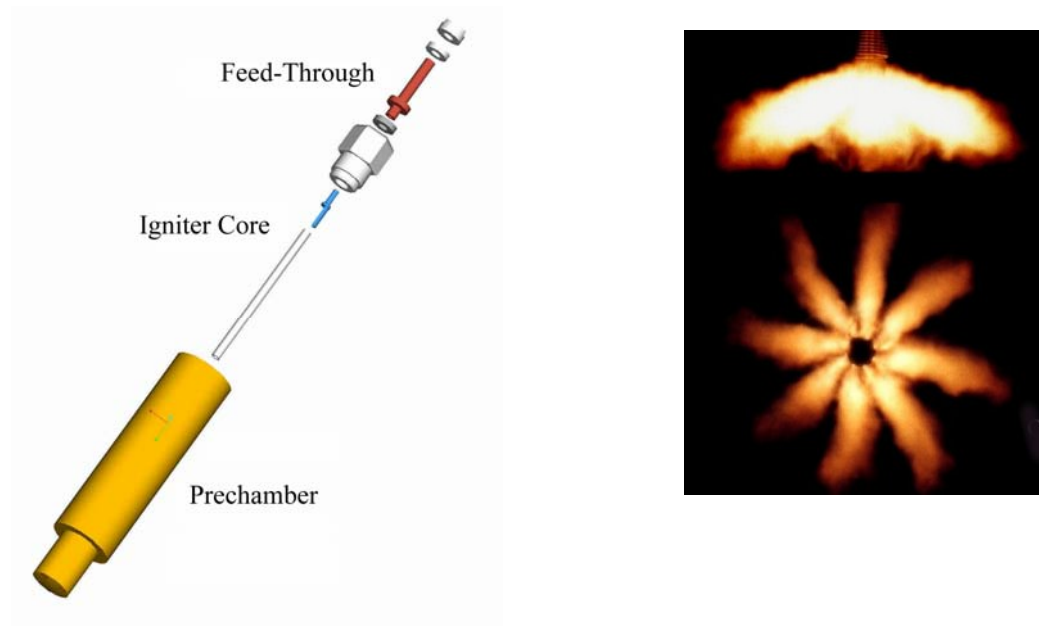


Figure 1.3 Components of the ARI catalytic igniter and flame exiting the pre-chamber.

1.4 Modal Testing

A primary thrust of this research was to accommodate a test protocol that would allow local testing of the vehicle that would mimic the FTP driving cycles. Approximating a FTP driving cycle allows the fuel mapping and exhaust after treatment to be evaluated and modified for best possible vehicle emissions and performance.

The FTP driving cycle is a speed-time trace that a vehicle must follow while a transient chassis dynamometer mimics road power requirements. The FTP-72 trace imitates city driving, and is shown in Figure 1.4.1, while the Highway Fuel Economy Test (HWFET) is shown in Figure 1.4.2. With no transient dynamometer existing in the Northwest, an approximation using the steady-state chassis dynamometer was used. A six-mode test was created to collect data at four steady state points and two mock-acceleration points. These are shown in Table 1.4. To estimate driving cycle performance, weighting factors are applied to each data point representing percent time of each point in the FTP-72 and HWFET driving cycles. Other countries still use weighted steady-state modal tests for new vehicle certification [Gunther, 1999].

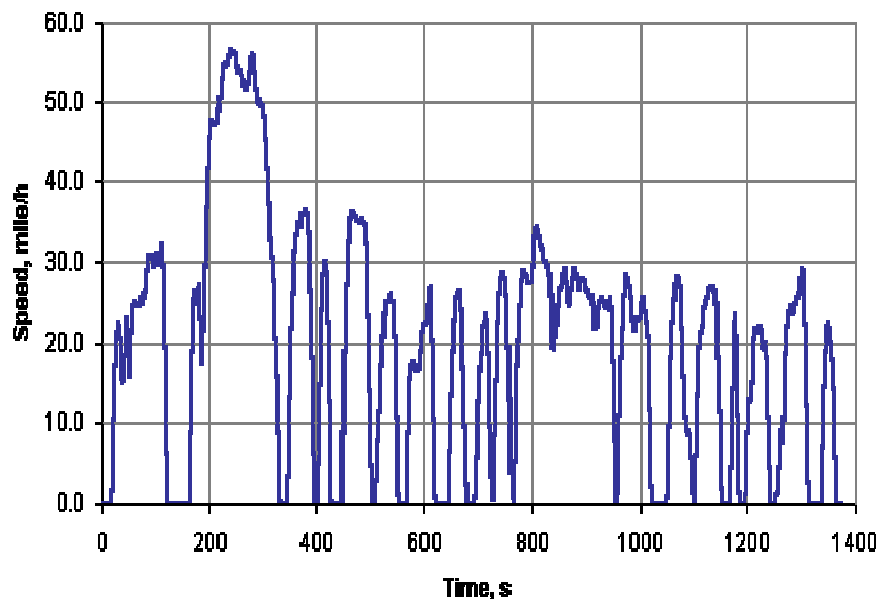


Figure 1.4.1 FTP Urban driving cycle

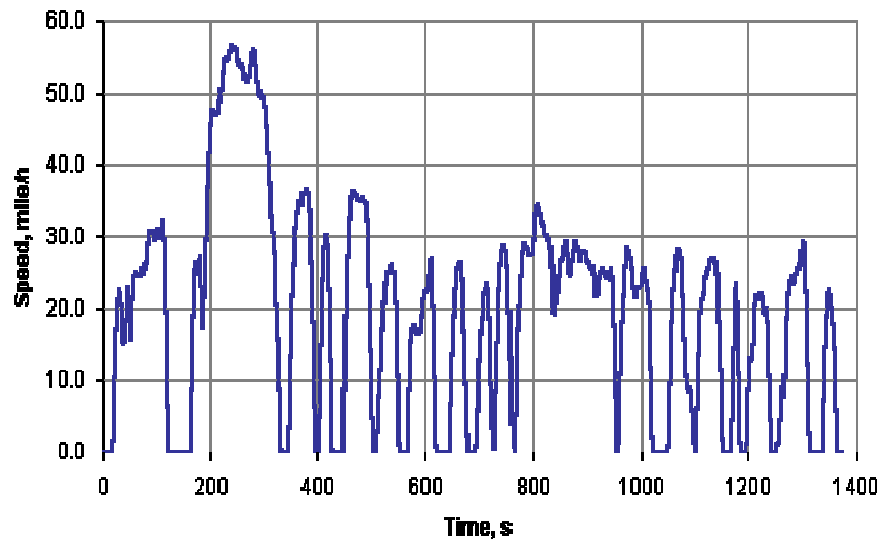


Figure 1.4.2 Highway driving cycle

Table 1.4 Description of the 6-mode points with weighting factors

Mode	Speed	Load	Weighting Factor
1	Idle	---	0.05
2	25 mph	Road Load	0.35
3	20 mph	50% throttle	0.15
4	45 mph	Road Load	0.25
5	40 mph	50% throttle	0.10
6	60 mph	Road Load	0.10

2 RESEARCH INFRASTRUCTURE

Chapter 2 discusses the experimental equipment used to obtain performance and emissions data. Information regarding dynamometer safety and operation is given in the form of an abbreviated instruction manual. Modifications to aid in cold-starting and special maintenance procedures are discussed as is the protocol for multi-mode testing.

2.1 Dynamometer Facility

Performance and emissions comparisons were made on a SuperFlow model SF602 steady-state chassis dynamometer located in the J. Martin Laboratory at the University of Idaho. As a “Truck Chassis Dynamometer,” the SF602 allows operation of a wide range of power and speed modes and performs a critical role in testing equipment for this research. Figure 2.1.1 shows a rendering of the chassis dynamometer and experimental equipment used during testing. The SF602 is capable of absorbing 550 horsepower from each of two three foot diameter rolls at a maximum test speed of 80 mph [SuperFlow Operators Manual, 1998]. Load is controlled during testing by a pneumatic valve that controls water flow into a water break absorber attached to the roll. A handheld controller can be set to monitor and change the water flow based on a variety of control parameters including wheel speed and percent flow.

The SF602 has been installed in the J. Martin Laboratory in a sub floor configuration. Steel plates covering the rolls and wheel channels must be removed and safely stored using a forklift before a vehicle can be loaded on the rolls. Removal of the steel plates can be done in about a ½ hour with two people. Figures 2.1.2 and 2.1.3 show proper removal of the floor plates using the forklift and fork attached removal tools.

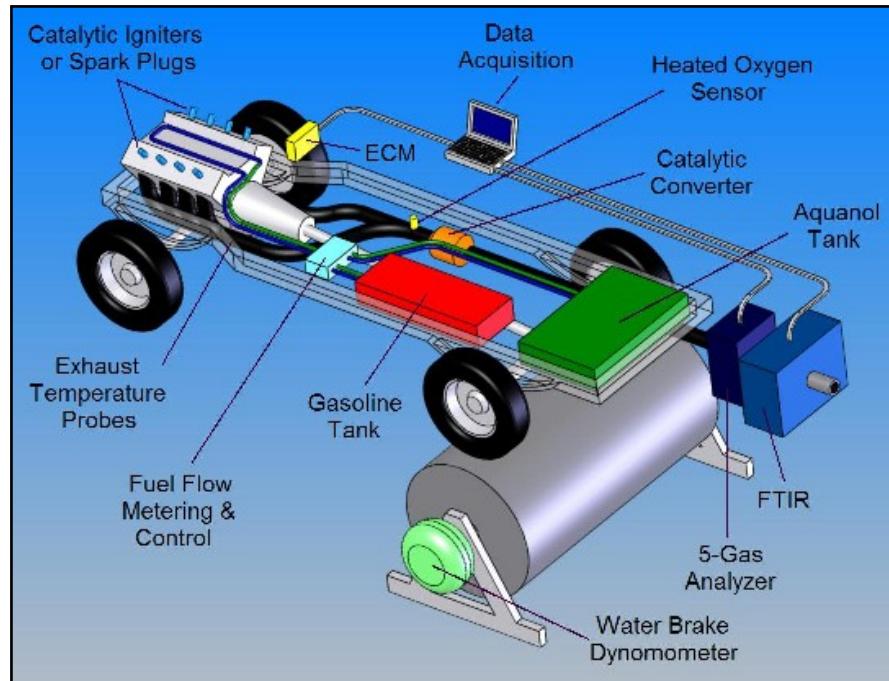


Figure 2.1.1 Experimental Equipment used during dynamometer testing.



FIGURE 2.1.2 Removal of the roll cover floor plates using forklift.



FIGURE 2.1.3 Removal of the smaller tie-down track floor plates using forklift

The tie down track floor plates must be stored in the rack outside of the bay to prevent them from shifting or falling. The tie down track floor plates do not stack horizontally because of the support lug on the bottom and improper storage could cause injury if they were to fall on an operator or observer. Figure 2.1.4 shows the rack to be used.



Figure 2.1.4 Rack to store tie down track floor plates.

Another consideration to be aware of when removing the plates is the order in which they must be re-installed. Figure 2.1.5 shows the order of removal/installation as well as the correct location of each numbered plate. Plate numbers are scribed on the underside of each plate next to the lift holes.



Figure 2.1.5 Proper location of dynamometer floor plates and order of removal/installation.

With the SF602 system power on, the vehicle chassis should be centered and backed onto the rolls. It is necessary to have the rolls in the locked configuration on the handheld controller to prevent them from spinning and ensure proper chassis alignment. In the final testing configuration, the wheels should be located forward of the center of the rolls. The following three-step procedure outlines how to obtain proper chassis positioning:

1. Back the vehicle onto the rolls so that the tire centers and roll centers are vertically aligned.
2. Attach the chain between the floor anchor and the differential housing only. (This is important not only because of strength and safety, but also to minimize vibration during operation.) Avoid crushing the brake lines that run on the axle housing when the chain becomes tight. Figure 2.1.6 shows correct attachment of the chain to the differential housing.
3. With approximately one foot of slack in the attached chain, allow the vehicle to roll forward until the rear tires stop forward of roll centers but clear of the floor with the chain taught.

Figure 2.1.7 shows the van properly positioned for testing on the dynamometer rolls. After correct positioning is obtained, the vehicle's front wheels are secured to the floor using the ratchet straps and tie-down chains illustrated in figure 2.1.8.



Figure 2.1.6 Correct attachment of the chain to the differential housing.



Figure 2.1.7 Correct location of rear wheel with respect to roll center



Figure 2.1.8 Ratchet straps and chains securing front wheels.

Operation and preparation of the chassis dynamometer should only be performed with two or more persons present. The following checklist should be observed before running the vehicle for safety and quality of testing:

1. Front tire ratchet straps and the rear differential mount chain are securely attached and tightly bound.
2. Dynamometer rolls are clear of tools, equipment, hoses and cables, or anything that could become caught during operation.
3. Exhaust ducting is attached to tailpipe and exhaust fan is on (Figure 2.1.9).
4. Patton Industrial fan is positioned in front of vehicle to pull fresh air from open bay door and cool radiator (Figure 2.1.10).



Figure 2.1.9 Exhaust ducting attached to tailpipe

Once the vehicle's front tires are secured to the floor, avoid turning the steering wheel to prevent loosening the ratchet straps. Secondly, when the rolls are spinning, avoid touching the brake pedal or locking the rolls with the handheld controller until they have come to a complete stop.



Figure 2.1.10 Patton industrial fan positioned in front of radiator to increase air flow.

2.2 Cold Starting Modifications

Cold starting capabilities of Aquanol fueled engines are generally poor. Indeed, in most reported cases, ethanol fueled engines with minimum water content must be started on a pilot fuel [Jehlik, 1999]. In an attempt to cold-start on Aquanol alone, a number of modifications were made to the engine and platform. Most significantly, a 600 watt *Napa* in-line radiator heater was installed on the lower radiator hose and is capable of increasing engine temperature from 70 to 105 degrees Fahrenheit in three to four hours. This procedure requires the vehicle to be located near a power outlet prior to functioning but is critical for reliable starting on Aquanol in this vehicle. The radiator heater used in the van is shown in Figure 2.2.1.

Cold-starting ability is also improved by pre-heating the catalytic igniters for two minutes before starting. The catalytic igniters, unlike conventional spark plugs, are not timed by the distributor and are powered whenever the key is in the run position. To prevent the on-board battery from depleting during catalytic igniter pre-heating, a battery charger should be attached, maintaining two amps to the battery posts.



Figure 2.2.1 600 Watt Napa in-line radiator heater.

If insufficient time is available before testing to allow the engine temperature to reach 105 degrees Fahrenheit, ether may be sprayed in small quantities into the intake without harming the catalytic igniters and has shown increased cold-starting potential.

2.3 Injector Maintenance

One of the major systems unique to a dual-fuel vehicle is the fuel handling system. Because gasoline is the predominant fuel used in the U.S., nearly all fuel system components have been designed to be compatible with gasoline. Alcohol fuels, especially when combined with water, are significantly more corrosive than gasoline and typical fuel handling components are susceptible to rapid corrosion when used with Aquanol and not properly maintained.

To extend the life of fuel injectors used in this platform, a flushing and maintenance procedure was developed. When the time between test runs was less than 48 hours, it was sufficient to flush the system with gasoline from the onboard tank by simple switching the fuel path at the valve bank and allowing gasoline to purge the system at the end of a test run. This procedure had the dual effect of clearing the injectors of corrosive fuel, as

well as leaving a small amount of gasoline in the system to act as a pilot fuel during the next cold-start. When time between test runs was to exceed 48 hours, the fuel-injectors were removed and flushed through the unit shown in Figure 2.3.1 below.

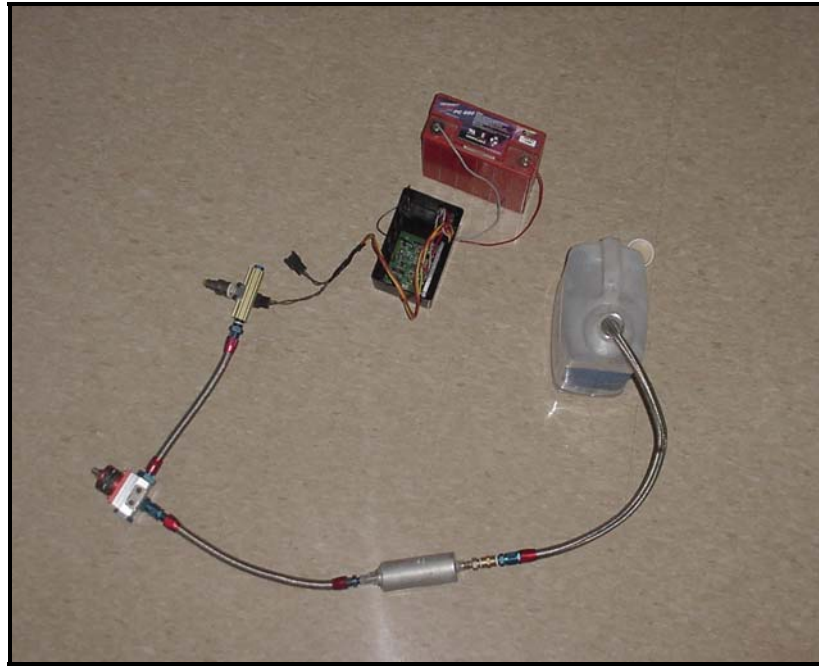


Figure 2.3.1 Backflushing unit

Using a variable pulse circuit and DC power supply, the fuel-injector flushing unit back-flushes the fuel injectors with STP injector cleaner. Pressurized air is used to force the STP injector cleaner through the fuel-injector spray ports at 30 psi.

3 EXPERIMENTAL DESIGN

The objective of this research was to use test protocols involving a steady-state dynamometer to rigorously evaluate vehicle performance and emissions under six modal conditions. Comparisons were made in the dual-fuel transit van on both gasoline and Aquanol. The performance parameters used to compare the two fuels were throttle position, wheel speed, torque, horsepower, and fuel rate. The emissions parameters used to compare the two fuels were CO₂, CO, NO, HC.

To meet the objectives of this research, equipment shown in Figure 2.1.1 was assembled to give accurate results under the six modal conditions. In addition, an optical pyrometer was used to monitor cylinder temperature. This is described in Section 3.1 along with typical engine coolant temperatures. Section 3.2 discusses the fuel maps used in this research. Section 3.3 explains how to replicate road load conditions on the chassis dynamometer. Section 3.4 outlines the exhaust monitoring equipment and calibration procedure. Section 3.5 describes how fuel metering was conducted.

3.1 Optical Pyrometer

An infrared pyrometer was used to verify that all cylinders were running with consistent fuel ignition and fuel delivery through the injectors. Temperatures were to establish relative comparisons only as there was no surface emissivity correction taken into account for absolute temperatures. Eight temperatures were taken on the exhaust headers two inches downstream of the engine heads. Tables 3.1.1 and 3.1.2 show typical temperatures under operating conditions when engine coolant temperatures peaked at about 195 degrees Fahrenheit.

Table 3.1.1 Typical header temperatures during operation on gasoline.

Driver Cylinder Bank		Passenger Cylinder Bank	
Cylinder No	Pyrometer Temp (F)	Cylinder No	Pyrometer Temp (F)
5	976	4	910
6	1018	3	998
7	1076	2	960
8	950	1	1000

**Table 3.1.2 Typical header temperatures during operation on Aquanol
(90/10)**

Driver Cylinder Bank		Passenger Cylinder Bank	
Cylinder No	Pyrometer Temp (F)	Cylinder No	Pyrometer Temp (F)
5	603	4	550
6	586	3	524
7	632	2	595
8	616	1	610

The optical pyrometer was also used to determine catalytic converter temperatures and compare to manufacturer light-off temperatures. As expected, header temperatures experienced during operation on Aquanol are significantly lower than with those temperatures associated with gasoline. Aquanol header temperatures are also significantly lower than manufacturer light-off temperatures.

3.2 Fuel Maps

The fuel maps were programmed into the onboard electronic control unit (ECU) through a laptop computer. Using this method fuel flow duration can be adjusted during dynamometer operation or over-the-road driving, allowing for quick response and feedback. Figure 3.2.1 below shows a typical 3-D fuel map for Aquanol under start-up conditions. The x-axis represents the duration of fuel flow in milliseconds. The y-axis represents the load in inches of mercury. The z-axis represents engine speed from 0 to 5500 rpm. In addition to controlling fuel flow, manifold pressure, coolant temperature, air temperature, and battery voltage can be monitored through the ECU.

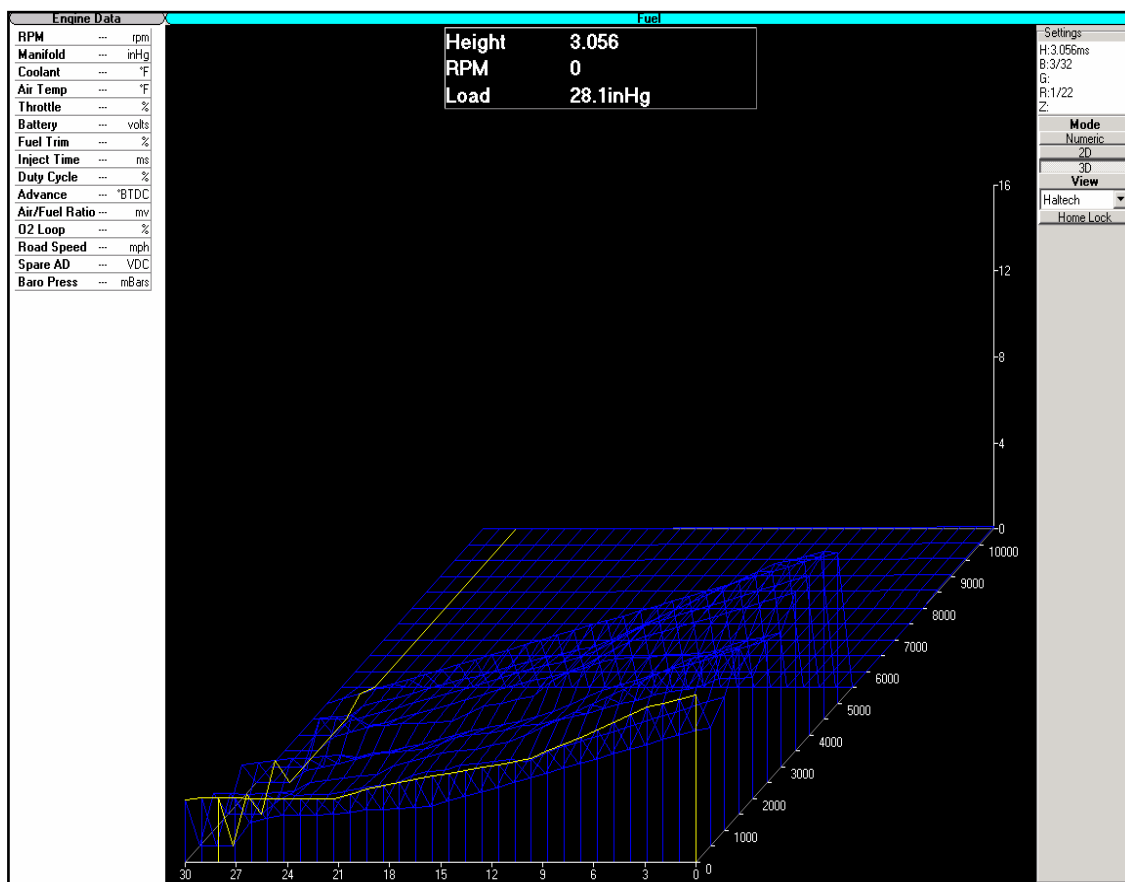


Figure 3.2.1. 3-D fuel injector maps from start-up to 5500 rpm.

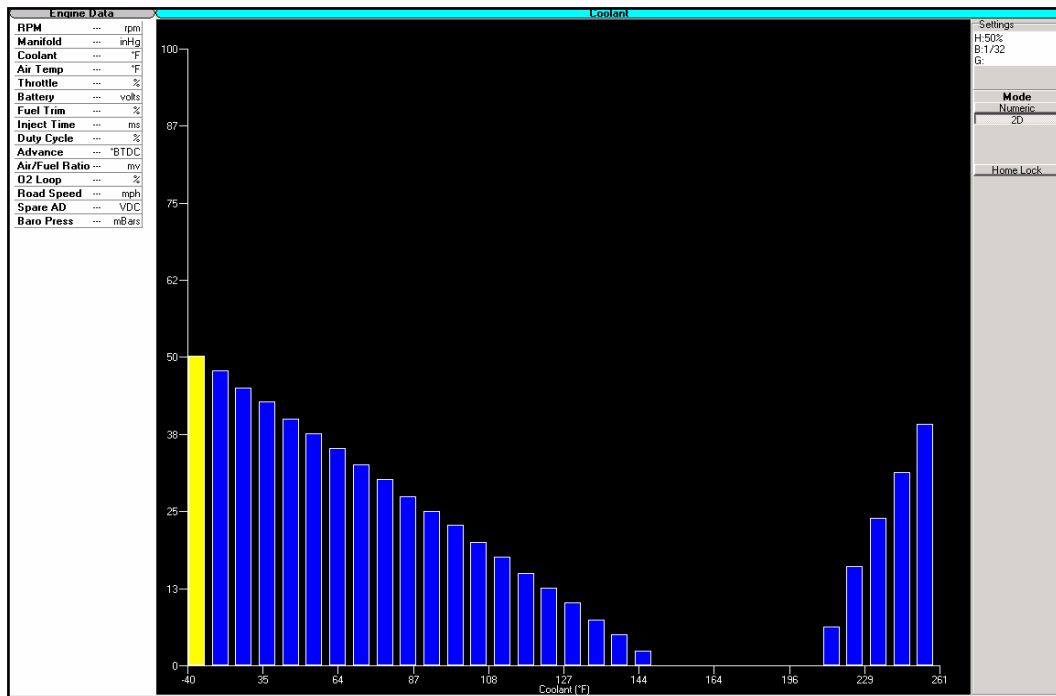


Figure 3.2.2. Fuel injector duration with respect to coolant temperature.

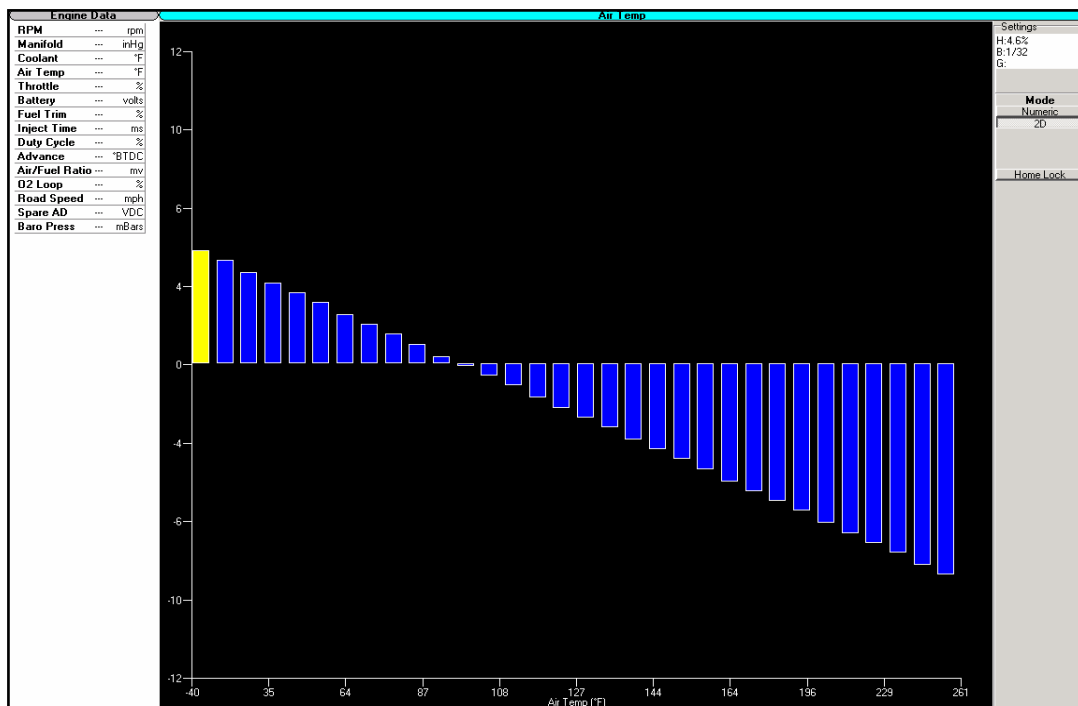


Figure 3.2.3. Fuel injector duration with respect to air temperature.

Engine Data			Fuel																										Settings		
			30.0	29.1	28.1	27.1	26.1	25.2	24.2	23.2	22.2	21.3	20.4	19.4	18.4	17.4	16.5	15.5	14.5	13.5	12.6	11.6	10.6	9.6	8.7						
RPM	---	rpm																									H:3.056ms B:3/32 G: R:1/22 Z:				
Manifold	---	inHg	0	2.992	3.056	3.056	3.056	3.040	3.040	3.024	3.024	3.008	3.248	3.504	3.664	3.808	3.952	4.096	4.240	4.368	4.512	4.656	4.800	4.944	5.296						
Coolant	---	°F	500	0.016	0.000	0.000	1.120	1.280	1.472	1.440	1.456	1.520	1.552	1.696	1.744	1.792	1.824	1.888	2.112	2.336	2.560	2.784	3.008	3.232	3.456	3.680					
Air Temp	---	°F	1000	1.760	1.760	1.744	1.760	1.840	1.664	1.696	1.696	1.856	2.032	2.112	2.224	2.624	2.816	2.880	3.120	3.184	3.264	3.408	3.264	3.632	3.936	4.176					
Throttle	---	%	1500	0.000	0.000	0.000	0.640	1.072	1.520	1.616	1.744	1.808	1.856	2.272	2.512	2.720	2.928	3.008	3.056	3.264	3.456	3.760	4.128	4.496	4.864	5.216					
Battery	---	volts	2000	1.600	1.728	1.808	1.904	1.952	2.016	2.064	1.984	2.192	2.192	2.304	2.352	2.608	2.944	3.088	3.136	3.296	3.472	3.568	3.728	3.920	4.064	4.304					
Fuel Trim	---	%	2500	0.000	0.000	0.000	0.576	0.752	0.912	1.088	1.296	1.472	1.680	1.840	2.048	2.240	2.432	2.608	2.784	2.944	3.120	3.392	3.712	4.048	4.384	4.624					
Inject Time	---	ms	3000	0.000	0.000	0.000	2.368	2.400	2.432	1.968	1.968	2.064	2.080	2.160	2.208	2.576	2.896	3.024	3.248	3.392	4.048	4.496	4.688	5.024	5.168	5.216					
Duty Cycle	---	%	3500	0.000	0.000	0.000	0.688	0.896	1.072	1.312	1.552	1.776	2.000	2.192	2.432	2.656	2.896	3.104	3.312	3.504	3.712	4.032	4.432	4.832	5.232	5.456					
Advance	---	°BTDC	4000	0.000	0.000	0.000	0.688	0.896	1.072	1.312	1.552	1.776	2.000	2.192	2.432	2.656	2.896	3.104	3.312	3.504	3.712	4.032	4.432	4.832	5.232	5.472					
Air/Fuel Ratio	---	mv	4500	0.000	0.000	0.000	0.640	0.832	1.008	1.216	1.440	1.648	1.856	2.048	2.272	2.480	2.688	2.896	3.088	3.264	3.456	3.760	4.128	4.496	4.864	5.216					
O2 Loop	---	%	5000	0.000	0.240	0.464	0.704	0.928	1.168	1.392	1.632	1.856	2.096	2.320	2.560	2.800	3.024	3.264	3.488	3.728	3.952	4.192	4.416	4.656	4.896	5.120					
Road Speed	---	mph	5500	0.000	0.000	0.000	0.000	0.000	0.000	0.000	0.000	0.000	0.000	0.000	0.000	0.000	0.000	0.000	0.000	0.000	0.000	0.000	0.000	0.000	0.000	0.000					
Spare AD	---	VDC	6000	0.000	0.000	0.000	0.000	0.000	0.000	0.000	0.000	0.000	0.000	0.000	0.000	0.000	0.000	0.000	0.000	0.000	0.000	0.000	0.000	0.000	0.000	0.000					
Baro Press	---	mBars	6500	0.000	0.000	0.000	0.000	0.000	0.000	0.000	0.000	0.000	0.000	0.000	0.000	0.000	0.000	0.000	0.000	0.000	0.000	0.000	0.000	0.000	0.000	0.000					
			7000	0.000	0.000	0.000	0.000	0.000	0.000	0.000	0.000	0.000	0.000	0.000	0.000	0.000	0.000	0.000	0.000	0.000	0.000	0.000	0.000	0.000	0.000	0.000					
			7500	0.000	0.000	0.000	0.000	0.000	0.000	0.000	0.000	0.000	0.000	0.000	0.000	0.000	0.000	0.000	0.000	0.000	0.000	0.000	0.000	0.000	0.000	0.000					
			8000	0.000	0.000	0.000	0.000	0.000	0.000	0.000	0.000	0.000	0.000	0.000	0.000	0.000	0.000	0.000	0.000	0.000	0.000	0.000	0.000	0.000	0.000	0.000					
			8500	0.000	0.000	0.000	0.000	0.016	0.016	0.016	0.016	0.016	0.016	0.016	0.016	0.016	0.032	0.032	0.032	0.032	0.032	0.032	0.048	0.048	0.048	0.048					
			9000	0.000	0.000	0.000	0.000	0.016	0.016	0.016	0.016	0.016	0.016	0.016	0.016	0.016	0.032	0.032	0.032	0.032	0.032	0.032	0.048	0.048	0.048	0.048					
			9500	0.000	0.000	0.000	0.000	0.016	0.016	0.016	0.016	0.016	0.016	0.016	0.016	0.016	0.032	0.032	0.032	0.032	0.032	0.032	0.048	0.048	0.048	0.048					
			10000	0.000	0.000	0.000	0.000	0.016	0.000	0.016	0.016	0.016	0.016	0.016	0.016	0.016	0.032	0.032	0.032	0.032	0.032	0.032	0.048	0.048	0.048	0.048					
			10500	0.000	0.000	0.000	0.000	0.016	0.016	0.016	0.016	0.016	0.016	0.016	0.016	0.016	0.032	0.032	0.032	0.032	0.032	0.032	0.048	0.048	0.048	0.048					

Figure 3.2.4. Tabular representation of fuel map.

3.3 Road Load Replication

Since performance measurements were dependent on the inputs of dynamometer speed control and vehicle throttle position, a procedure was developed to calibrate wheel speeds. First, a road test was performed. Throttle position readings were taken from an onboard programmable control module while vehicle speed was calibrated as compared to speed read from a Garmin E-trex GPS with accuracy of +/- 0.1 mph. The van was then run on the chassis dynamometer under no load conditions. Six calibrated speeds taken from the road tests were compared to the dynamometer speed readings, giving a correction factor on the dynamometer wheel speed. The corrected dynamometer wheel speed along with throttle positions determined from the road tests then became the input.

The dynamometer's speed control was set to the six modal points and the matching throttle positions were held constant. When steady-state was reached, a torque reading measured at the wheels was recorded.

3.4 Exhaust Measurements

Exhaust gas species were recorded using an EMS model 5001 five-gas analyzer. Emissions were recorded about 15 inches from the output of the tailpipe. Although transient response of this unit is slow, achieving steady state conditions is constrained by the dynamometers speed control not the five-gas analyzer. The five-gas analyzer has the ability to accurately measure CO₂, CO, NO_x, O₂, and HC's. The five-gas analyzer is not capable of measuring aldehyde emissions.

To ensure the accuracy of measured emissions, the five-gas analyzer must be calibrated on a regular basis. The manufacturer recommends calibration every three months using a known mixture of gases called 'cal-gas'. If the concentrations recorded by the five-gas analyzer match those being supplied by the cal-gas tank further calibration is unnecessary. Table 3.4.1 shows the composition of the calibration gases used.

Table 3.4.1 Composition of calibration gas.

Propane	202 ppm
NO	298 ppm
CO	0.5 %
CO ₂	6.05 %
Nitrogen	Balance

3.5 Fuel Metering

The MAX Machinery 710 series positive displacement fuel metering system shown in figure 3.5 was used to monitor fuel consumption. Also shown is the remote fuel tank and fuel metering box that monitor both the feed and the return lines from the engine.



Figure 3.5 MAX Machinery 710 fuel metering system

4 RESULTS

At this time, chassis dynamometer data has been collected on gasoline and Aquanol (90/10) and extensive baseline fuel mapping has been performed. Table 4.0.1 documents errors attributable to each piece of test equipment. Section 4.1 explores differences in engine performance. Similarly, section 4.2 explores differences in exhaust emissions.

Table 4.0.1 Measurement Errors for Data Collection Equipment

TEST EQUIPMENT		ERROR
TORQUE and HORSEPOWER		1-2%
FIVE-GAS ANALYZER	CO ₂	.5 %
	CO	.5 %
	Nox	25 PPM
	HC	25 PPM
FUEL METER		0.1 GPH
PYROMETER		5 F
HALTEC	Engine temperature	10 F
	Throttle position	2 %

4.1 Performance Testing

Performance was measured at the wheels in terms of torque and horsepower. At modes three and five throttle position was the same for both fuels as defined by the six modes derived from the FTP Urban Driving Cycle. Readings in mode five were not obtained for operation on Aquanol. This was due to an inability to maintain a consistent dynamometer roll speed while still keeping up with the large fuel flow requirements at 50 percent throttle. Under the idle conditions represented by mode one, torque and horsepower were

negligible with any forces due only to inertia in the vehicle's drive train and the dynamometer rolls. Mode three shows a 31 percent decrease in torque and a 28 percent decrease in horsepower at 50 percent throttle position with a wheel speed of 20 mph for operation on Aquanol (90/10) versus gasoline. While the energy in Aquanol is more than 30 percent less than that in the same volume of gasoline, one must look at the increases in fuel flow as a result of fuel mapping and not at throttle position alone.

Under the road load conditions of modes two, four, and six, throttle position for Aquanol (90/10) is somewhat higher than gasoline. Here the six-mode approximation defines only wheel speed. The fuel needed to overcome road load forces at this speed are predictably more for operation on Aquanol (90/10) than on gasoline. Torque and horsepower reading were higher with Aquanol (90/10) than with gasoline in all three of these modes. Though a definitive conclusion cannot be drawn from such a small sampling of data, this increase in power does make sense. Mode six represents the highest throttle position at 15 percent for Aquanol (90/10).

The fuel injectors used in this testing were capable of maintaining required flows at 15 percent throttle so there was no loss of power due to insufficient fuel. As documented by the optical pyrometer data in Chapter 3, operating temperatures were significantly less during operation on Aquanol (90/10) than on gasoline. The increases in torque and horsepower may be the result of decreased engine temperature and increase engine rpm.

Table 4.1.1 Torque and horsepower over the six modal points.

MODE	FUEL	THROTTLE POSITION (%)	DYNO SPEED (MPH)	TORQUE (FT*LB)	HORSEPOWER
1	Gasoline	0	0	0	0
	Aquanol (90/10)	0	0	0	0
2	Gasoline	3	25	155	7
	Aquanol (90/10)	4	25	164	8
3	Gasoline	50	20	1823	62
	Aquanol (90/10)	50	20	1254	45
4	Gasoline	7	44	128	10
	Aquanol (90/10)	9	45	137	12
5	Gasoline	50	39	842	58
	Aquanol (90/10)	50	40	**	**
6	Gasoline	11	58	216	23
	Aquanol (90/10)	15	57	228	25

4.2 Emissions Testing

Table 4.2 below compares four major pollutant species over the six modes discussed in Table 1.4. CO₂ concentrations were on the order of 70 percent higher during Aquanol operation. This result is consistent with other studies involving alcohol based fuels [Cordon, 2002]. CO concentrations were on the order of 20 percent less during Aquanol

operation. Larger decreases in CO have been documented for engines burning Aquanol with water content above 20 percent [Morton, 1999] as increasing the fuels water content allows for more CO destruction by conversion to CO₂. Additionally, an increase in CO can be attributed to incomplete combustion at modes three and five, as the fuel maps were not designed to provide lean-burn conditions at these modes. NO_x production was on the order of 25 percent less during Aquanol (90/10) operation. Further decreases can be expected with increasing water content. A large increase in HC production was recorded during Aquanol (90/10) operation. The catalytic converters installed on the test platform never reached light-off temperatures during operation on Aquanol. However, both cylinder banks were well above light-off temperature during operation on gasoline. By adding a catalytic converter with lower light-off temperature, these differences should disappear.

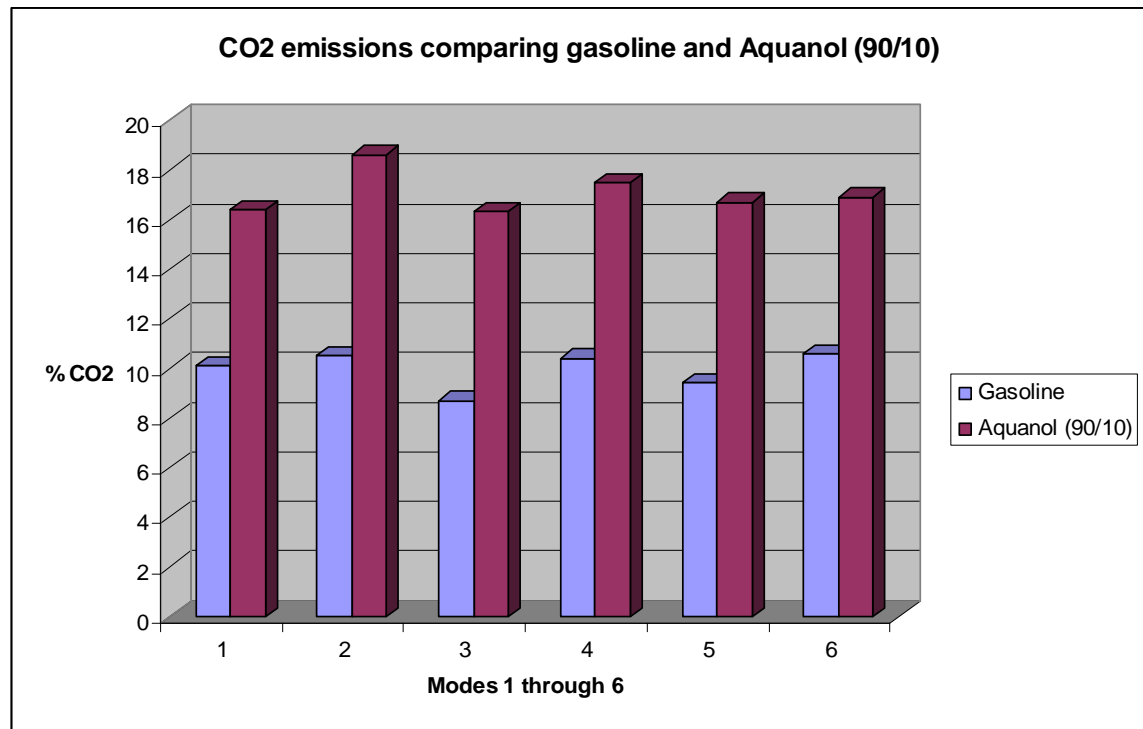


Figure 4.2.1 Bar chart comparing CO₂ emissions of gasoline and Aquanol (90/10).

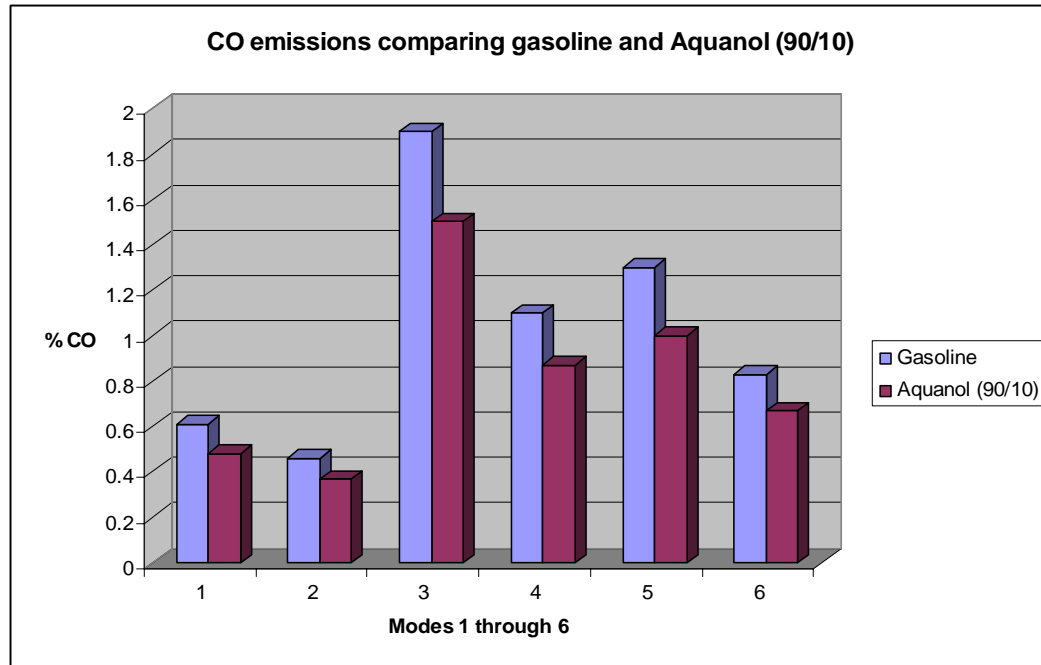


Figure 4.2.2 Bar chart comparing CO emissions of gasoline and Aquanol (90/10).

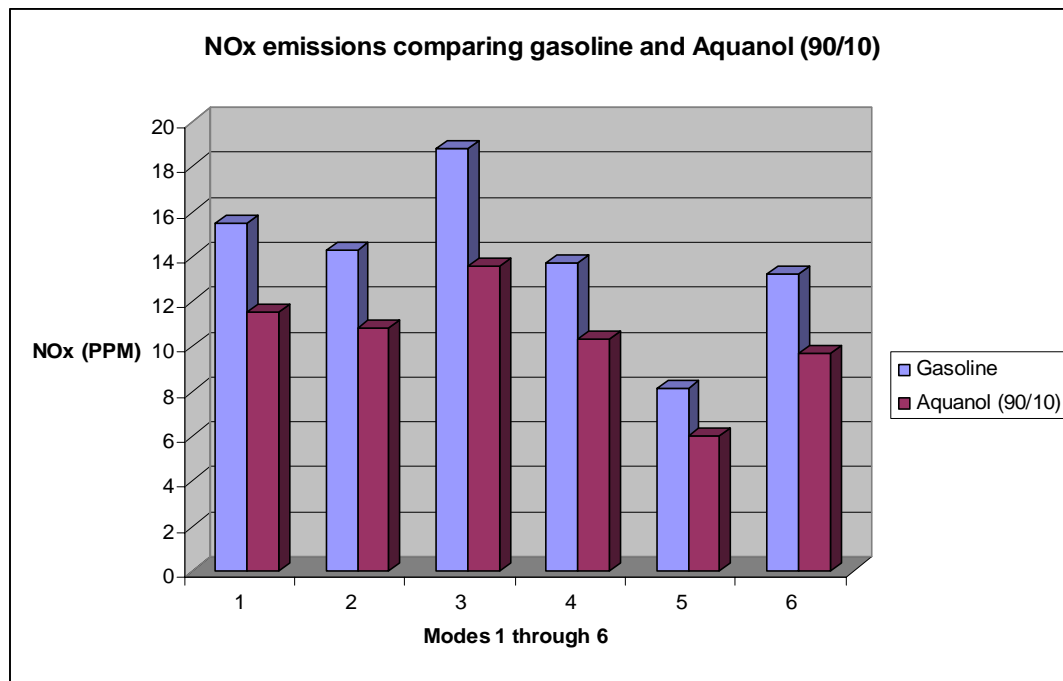


Figure 4.2.3 Bar chart comparing NOx emissions of gasoline and Aquanol (90/10).

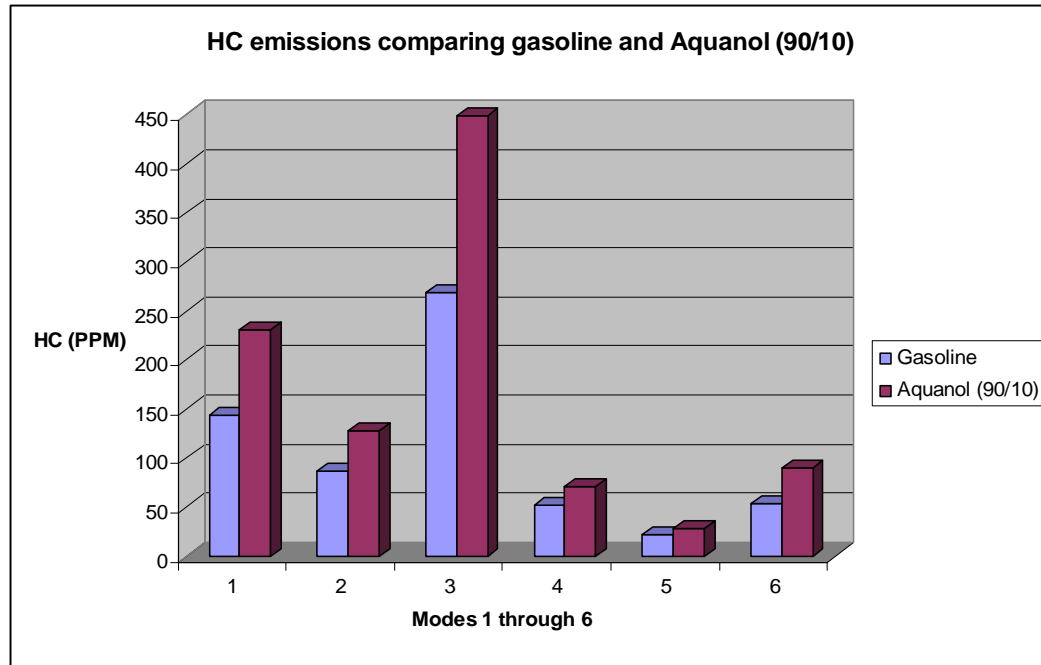


Figure 4.2.4 Bar chart comparing HC emissions of gasoline and Aquanol (90/10).

Table 4.2 five-gas emissions of Aquanol and gasoline over the six modal points.

MODE	FUEL	THROTTLE POSITION (%)	DYNO SPEED (MPH)	CO2 (%)	CO (%)	Nox (PPM)	HC (PPM)
1	Gasoline	0	0	10.1	0.61	15.5	143
	Aquanol (90/10)	0	0	16.4	0.48	11.5	231
2	Gasoline	3	25	10.5	0.46	14.3	86
	Aquanol (90/10)	4	25	18.6	0.37	10.8	127
3	Gasoline	50	20	8.7	1.9	18.8	268
	Aquanol (90/10)	50	20	16.3	1.5	13.6	449
4	Gasoline	7	44	10.4	1.1	13.7	52
	Aquanol (90/10)	9	45	17.5	0.87	10.3	71
5	Gasoline	50	39	9.4	1.3	8.1	22
	Aquanol (90/10)	50	40	16.7	1	6	28
6	Gasoline	11	58	10.6	0.83	13.2	53
	Aquanol (90/10)	15	57	16.9	0.67	9.7	90

5 CONCLUSIONS

This work has provided infrastructure for comparing performance and emissions data from a dual-fuel passenger van operating on Aquanol (90/10) versus gasoline. Major refinements to this platform included: (a) facilitating cold-starting on Aquanol (90/10) by installing an engine coolant heater and boosting igniter amperage; (b) insuring proper igniter performance by monitoring individual cylinder temperatures with an optical pyrometer; and (c) implementing a fuel injector flushing procedure to prevent long-term exposure to ethanol/water.

Fuel mapping is much more sophisticated than the approach used previously. Prior fuel maps were based on a constant off-set from gasoline maps. As part of this work, fuel maps were tuned specifically for Aquanol (90/10) in response to manifold pressure and engine speed.

This work has revealed a number of issues associated with alternative fuel testing that we did not anticipate. Test modes defined by wheel speed and throttle position do not account for differences in fuel energy content. At the same throttle position, operation on Aquanol (90/10) will produce considerably less power than gasoline. In addition to linear errors associated with performance and emissions data collection equipment, expected uncertainty will increase at higher load points. This can be attributed to increased settling time during dynamometer operation and difficulty in maintaining steady state operation under conditions requiring high heat rejection.

6 RECOMMENDATIONS

This section gives recommendations for more accurate dynamometer testing as well as more robust operation of the dual-fuel platform. These recommendations respond to lessons learned in data collection with the steady-state dynamometer, cold-starting issues, and better understanding of exhaust clean-up requirements.

6.1 Recommendations for test protocol

In this work, emissions data was collected using the five-gas analyzer discussed in section 3.4. Ethanol emissions, however, contain substantial levels of aldehydes especially acetaldehyde which cannot be detected by the five-gas analyzer [Mayotte, 1994]. To record the levels of aldehydes produced by this platform, a Fourier Transform Infrared Spectrometer (FTIR) should be used and is recommended in future work for more complete emission detection. This is the thrust of continuing work by Dan Cordon.

A major change in testing procedures should be a redesign of the modal comparison scheme. During dynamometer operation, it is advisable to keep high load runs to a minimum, allowing greater time spent collecting data without encountering engine overheating. Further, modes three and five should be eliminated because these refer to constant throttle positions which do not correspond to the same vehicle performance with different fuels.

6.1 Recommendations for dual-fuel platform

Hardware modifications to allow for realtime adjustment to the ethanol/water concentration entering the fuel injectors would improve the platform in many ways. Cold-starting would be improved by allowing for 100 percent ethanol to be used until the engine has reached operating temperature. Similarly, under high-load conditions, the water content could be decreased to allow for more power output at a lower throttle position. This would allow the fuel injectors to be sized with a more narrow operating range thus increasing their resolution and response. Over-the-road operation would

benefit by increased vehicle range and smoother acceleration. However, allowing for changing water concentrations would require separating the ethanol and water tanks and other hardware in the fuel handling system.

Another necessary hardware modification involves the catalytic exhaust cleanup. In the current configuration, exhaust created during operation on Aquanol (90/10) exits the vehicle without catalytic cleanup due to extremely low operating temperatures. Catalytic converters with reduced light-off temperatures or with an option to externally add heat may prove beneficial in exhaust cleanup.

REFERENCES

- Bradley, C., and K. Runnion, "Understanding Ethanol Fuel Production and Use." Volunteers in Technical Assistance, 1984.
- Cherry, M., R. Morrisset, and N. Beck, "Extending Lean Limit with Mass-Timed Compression Ignition Using a Plasma Torch," SAE Paper 921556, 1992.
- Cherry, M., Catalytic-Compression Timed Ignition, US Patent 5 109 817, December 18, 1990
- Clarke, E., "Characterization of Aqueous Ethanol Homogeneous Charge Catalytic Compression Ignition," Masters Thesis, University of Idaho, 2001.
- Cordon, D., E. Clarke, S. Beyerlein, J. Steciak, and M. Cherry, "Catalytic Igniter to Support Combustion of Ethanol-Water/Air Mixtures in Internal Combustion Engines," SAE Paper 02FFL-46, 2002.
- Cordon, D., "Multi-Fuel Platform and Test Protocols for Over-the-Road Evaluation of Catalytic Engine Technology," Masters Thesis, University of Idaho, 2001.
- Ethanol Report, U.S. Renewable Fuels Association, Issue # 76, July 2, 1998.
- Gottschalk, Mark A., "Catalytic Ignition Replaces Spark Plugs," *Design News*, May 22, 1995.
- Gunther, D., G. Konig, E. Schnaibel, D. Dambach, and W. Dieter, "Emissions Control Technology, Exhaust and Evaporative-Emissions Testing." *Gasoline-Engine Management*. 1999.
- Jehlik, F., M. Jones, P. Shepherd, J. Norbeck, K. Johnson, and M. McClanahan, "Development of a Low-Emission, Dedicated Ethanol-Fuel Vehicle with Cold-Start Distillation System," SAE Paper 1999-01-0611, 1999.

- Lee, W., and W. Geffers, "Engine Performance and Exhaust Emissions Characteristics of Spark Ignition Engines Burning Methanol and Methanol Mixtures," A.I.Ch.E. Symposium Series #165, Vol. 73, 1977.
- Mayotte, S.C., C. E. Lindhjem, V. Rao, and M. S. Sklar, "Reformulated Gasoline Effects on Exhaust Emissions: Phase I: Initial Investigation of Oxygenate, Volatility, Distillation, and Sulfur Effects," SAE Paper 941973, 1994
- Morton, A., M. Genoveva, S. Beyerlein, J. Steciak, and M. Cherry, "Aqueous Ethanol-Fueled Catalytic Ignition Engine," SAE Paper 1999-01-3267, 1999.
- Nadkarni, R. A., *Guide to ASTM Test Methods for the Analysis of Petroleum Products and Lubricants*, ASTM Publishing, West Conshohocken, PA, 2000
- Solomons, T. W. G., *Organic Chemistry*. New York: John Wiley and Sons, 1976.
- SuperFlow 602 Owner's Manual, Version 2, "Computerized Engine and Vehicle Test Systems." 1998.
- Wyman, C. E., *Handbook on Bioethanol, Production and Utilization*, National Renewable Energy Laboratory, NICH Report 24267 (424), 1996.